Vasoactive Intestinal Peptide, Forskolin, and Genistein Increase Apical CFTR Trafficking in the Rectal Gland of the Spiny Dogfish, *Squalus acanthias*

Acute Regulation of CFTR Trafficking in an Intact Epithelium

Rüdiger W. Lehrich,*§¶ Stephen G. Aller,*¶ Paul Webster,‡ Christopher R. Marino,‖ and John N. Forrest, Jr.*¶

**Department of Medicine and ‡Department of Cell Biology, Yale University School of Medicine, New Haven, Connecticut 06510; §Franz Volhard Clinic, Max Delbrück Center for Molecular Medicine, Virchow Klinikum, Humboldt University, 13122 Berlin, Germany; ‖Department of Medicine and Department of Physiology and Biophysics, University of Tennessee and Veterans Affairs Medical Center, Memphis, Tennessee 38104; and ¶Mount Desert Island Biological Laboratory, Salisbury Cove, Maine 04672*

Abstract

Defective trafficking of the cystic fibrosis transmembrane conductance regulator (CFTR) is the most common cause of cystic fibrosis. In chloride-secreting epithelia, it is well established that CFTR localizes to intracellular organelles and to apical membranes. However, it is controversial whether secretagogues regulate the trafficking of CFTR. To investigate whether acute hormonal stimulation of chloride secretion is coupled to the trafficking of CFTR, we used the intact shark rectal gland, a model tissue in which salt secretion is dynamically regulated and both chloride secretion and cellular CFTR immunofluorescence can be quantified in parallel. In rectal glands perfused under basal conditions without secretagogues, Cl^- secretion was 151±65 μeq/h/g. Vasoactive intestinal peptide (VIP), forskolin, and genistein led to 10-, 6-, and 4-fold increases in Cl^- secretion. In basal glands, quantitative confocal microscopy revealed CFTR immunofluorescence extending from the apical membrane deeply into the cell (7.28±0.35 μm). During stimulation with secretagogues, apical extension of CFTR immunofluorescence into the cell was reduced significantly to 3.24±0.08 μm by VIP, 4.08±0.13 by forskolin, and 3.19±0.1 by genistein ($P < 0.001$). Moreover, the peak intensity of CFTR fluorescence shifted towards the apical membrane (peak fluorescence 2.5±0.13 μm basal vs. 1.51±0.06, 1.77±0.1, and 1.38±0.05 for VIP, forskolin, and genistein; all $P < 0.001$). The increase in both Cl^- secretion and apical CFTR trafficking reversed to basal values after removal of VIP. These data provide the first quantitative morphological evidence for acute hormonal regulation of CFTR trafficking in an intact epithelial tissue. (*J. Clin. Invest.* 1998. 101:737–745.) Key words: cystic fibrosis transmembrane conductance regulator • CFTR • shark rectal gland • membrane trafficking • forskolin • genistein

Address correspondence to Dr. John N. Forrest, Jr., Department of Internal Medicine, Yale University School of Medicine, New Haven, CT 06510. Phone: 203-785-6633; FAX: 203-785-3234; E-mail: john.forrest@yale.edu

Received for publication 4 June 1997 and accepted in revised form 8 December 1997.

The Journal of Clinical Investigation
Volume 101, Number 4, February 1998, 737–745
http://www.jci.org

Introduction

Cystic fibrosis, the most common lethal genetic disease affecting Caucasians, is caused by mutations in the gene encoding for the cystic fibrosis transmembrane conductance regulator (CFTR)[1] (1). The most common mutation, ΔF508, is incompletely processed in the endoplasmic reticulum, resulting in a failure to translocate fully glycosylated CFTR to the plasma membrane (2, 3). Wild-type CFTR immunolocalizes to apical membranes in sweat glands, pancreatic ducts, airway cells, and T84 cells (2, 4, 5), and to intracellular organelles and subapical vesicles (6, 7), whereas the ΔF508 mutant is undetectable in apical membranes and is observed only as granular intracellular labeling (2, 3).

Several groups have suggested that CFTR trafficking is regulated by cAMP-dependent secretagogues. In pancreatic adenocarcinoma cells transfected with wild-type CFTR, Bradbury et al. (8) found that elevated cAMP levels inhibited endocytotic activity and increased the exocytosis of membrane vesicles, while cells expressing mutant CFTR failed to exhibit these responses. They first proposed that cAMP promotes the exocytotic insertion of CFTR into apical membranes. In human airway epithelial cell lines, Schwiebert et al. (9) showed that cAMP increases both Cl^- conductance and membrane capacitance and leads to the exocytosis of FITC-labeled, dextran-containing vesicles. However, in extensive studies using three cell lines expressing endogenous CFTR (T84 cells, Caco2, and HT29 clone 19A), maneuvers that increase cAMP (forskolin and 3-isobutyl-1-methyl xanthine) did not alter the labeling pattern for CFTR (10). In basal unstimulated T84 cells with biotin labeling of apical membrane CFTR, 50% of mature glycosylated CFTR was intracellular, with the remaining residing in the apical membrane; treatment with forskolin did not increase the relative amounts of CFTR in the apical membranes (11). Thus, it is controversial whether or not cAMP-dependent secretagogues acutely regulate the trafficking of CFTR. Currently, there is no morphological evidence in native tissue that CFTR trafficking from intracellular compartments to the apical membrane occurs when Cl^- secretion is stimulated by secretagogues.

All previous studies examining this issue have used monolayers of established cell lines expressing endogenous or transfected CFTR (8–13). We investigated this question in an intact

1. *Abbreviations used in this paper:* CFTR, cystic fibrosis transmembrane conductance regulator; VIP, vasoactive intestinal peptide.

epithelial organ, the rectal gland of the spiny dogfish shark, *Squalus acanthias.* The rectal gland is composed of secretory tubules of a single cell type that are highly specialized for acute, hormone-stimulated chloride secretion (14, 15). Chloride enters rectal gland tubular cells through a basolateral bumetanide-sensitive Na-K-2Cl cotransporter (16, 17) and exits through apical CFTR-like chloride channels. Shark CFTR is 72% identical to human CFTR (18), is regulated by cAMP, and has similar biophysical characteristics (19). The gland provides an ideal alternative model for investigating the possible coupling of CFTR trafficking to hormonal stimulation because of the ease of in vitro perfusion, its cellular homogeneity, the high activity of membrane transporters and channels, and the dynamic regulation of the gland by secretagogues. Parallel measurements of chloride secretion and quantitative measurements of CFTR immunofluorescence were carried out in each experiment, and studies were performed with secretagogues acting at different sites in signal transduction pathways regulating CFTR.

Methods

In vitro perfusion of shark rectal glands. Rectal glands were obtained from male dogfish sharks, *S. acanthias*, weighing 2–4 kg, which were caught by gill nets in Frenchman's Bay, ME, and kept in marine live cars until use, usually within 3 d of capture. Sharks were killed by pithing the spinal cord. Rectal glands were excised, and cannulae were placed in the artery, vein, and duct as described previously (20, 21). The rectal glands were then placed in a glass perfusion chamber maintained at 15°C with running sea water, and perfused with elasmobranch Ringer's solution containing 270 mM NaCl, 4 mM KCl, 3 mM $MgCl_2$, 2.5 mM $CaCl_2$, 1 mM KH_2PO_4, 8 mM $NaHCO_3$, 350 mM urea, 5 mM glucose, and 0.5 mM Na_2SO_4 (all from Sigma Chemical Co., St. Louis, MO), and equilibrated to pH 7.5 by bubbling with 99% O_2 and 1% CO_2. All glands were first perfused for 30 min in the absence of agonists to achieve basal levels of secretion. Measurements of duct flow and chloride secretion were made at 1-min intervals after the addition of secretagogues including vasoactive intestinal peptide (VIP) (Sigma Chemical Co.), forskolin (Calbiochem Corp., La Jolla, CA), or genistein (Calbiochem Corp.). Results are expressed as microequivalents of chloride secreted per hour per gram wet weight (μeq/h/g) ±SEM. For confocal microscopy, glands were frozen in liquid nitrogen immediately after the experiment.

Generation of R3195 CFTR antibodies. Antibodies against rodent CFTR were generated as described previously (4, 22). Briefly, a peptide (KEETEEEVQETRL) corresponding to the carboxy terminus of rodent CFTR was synthesized and HPLC-purified (Yale University Peptide Synthesis Facility). This peptide was conjugated to bovine thyroglobulin and used to immunize two rabbits (East Acres Biologicals, Inc., Southbridge, MA). Antiserum was then affinity-purified on a peptide column prepared by covalently linking the peptide to epoxy-activated Sepharose (Pharmacia Fine Chemicals, Inc., Piscataway, NJ). The antibodies were salt-eluted from the column, dialyzed, and concentrated using Aquacide II (Calbiochem Corp.).

Western blot analysis. Shark rectal glands were homogenized in lysis buffer containing 1% NP-40, 150 mM NaCl, 20 mM Tris base, pH 8.0, 5 mM EDTA, 10 mM NaF, 10 mM $Na_4P_2O_7$, 10 μg/ml aprotinin, 10 μg/ml leupeptin, 10 mM iodocetimide, 1 mM PMSF, and 1 mM sodium vanadate (all from Sigma Chemical Co.). The lysate was spun at 15,000 rpm/15 min. The protein concentration of the supernatant was determined, and the lysate was diluted in a 1:1 ratio with sample buffer containing 62.5 mM Tris HCl, pH 6.8, 2% SDS, 10% glycerol, 0.01% bromophenol blue, and 5% β-mercaptoethanol (all from Sigma Chemical Co.). Lysates were subjected to SDS-PAGE (7.5% acrylamide) and then electrotransferred to Immobilon® transfer membranes (Millipore Corp., Bedford, MA). Membranes were then probed with the rodent CFTR antibody and visualized with the enhanced chemiluminescence (ECL) detection system (DuPont-NEN, Wilmington, DE).

Specificity of R3195 CFTR antibody for shark CFTR. Separate studies were carried out in *Xenopus* oocytes to establish that the R3195 antibody specifically recognizes shark CFTR. Shark CFTR cRNA was prepared for oocyte injection as follows. A sense oligonucleotide primer was synthesized containing the T7 RNA polymerase promoter, a Kozak initiation sequence (23), and shark CFTR sequence, beginning at the start codon (18). The antisense oligo was designed from sequence immediately flanking the stop codon of shark CFTR. These primers were used in the PCR on shark rectal gland cDNA, using a mixture of Taq and Pwo thermostable polymerases (Stratagene Inc., La Jolla, CA). The reaction mixture was heated to 95°C for 1 min before adding the enzyme, and 28 cycles were performed at 95°C for 30 s, 55°C for 30 s, and 68°C for 4 min. The resulting 3871-bp product was extracted with phenol/chloroform and served as the template for cRNA synthesis. Capped messenger RNA was synthesized from the PCR product using T7 in vitro transcription (Ambion Inc., Austin, TX). Mature female *Xenopus laevis* were anesthetized in a 0.15% cold solution of tricane for 10 min, and several ovarian lobules were removed under sterile conditions through an abdominal incision. Oocytes were incubated in a 2.5-mg/ml solution of type I collagenase for ~ 2.5 h and subsequently manually defolliculated. Mature stage V and VI oocytes were selected and stored in modified Barth solution holding (MBSH) medium (88 mM NaCl, 1 mM KCl, 2.4 mM $NaHCO_3$, 0.82 mM $MgSO_4$, 0.33 mM $Ca(NO_3)_2$, 0.41 mM $CaCl_2$, 10 mM Hepes, and 150 mg/liter gentamicin sulfate (reagents from Sigma Chemical Co.). After 24 h, the oocytes were injected with 10 ng shark CFTR cRNA/50 nl or 50 nl of water and then stored for 2–3 d in MBSH at 18°C. Two-electrode voltage clamping of shark CFTR–injected oocytes, but not water-injected oocytes, had the electrophysiological characteristics of CFTR Cl^- channels (forskolin-stimulated increase in conductance, reduction in the reversal potential [V_{rev}] towards that of chloride, and sensitivity to glybenclamide [19] [data not shown]). Oocytes were then frozen in liquid nitrogen, cryosectioned, fixed in ice-cold acetone for 10 s, and labeled with CFTR antibody R3195. In control experiments, R3195 was preabsorbed with the peptide used to raise the antibody. Immunofluorescence of oocyte sections was performed as described above for sections of rectal gland tissue.

Confocal microscopy. Frozen perfused rectal glands were sectioned using a cryostat (2800 Frigocut E; Leica Inc., Deerfield, IL). Under each condition, 5–7-μm sections were obtained from the same region of the gland (2–3 mm from the distal tip). Sections were fixed for 10 s in ice-cold acetone or for 5 min in 4% paraformaldehyde at room temperature. Specimens were stored at −20°C. Before use, specimens were rehydrated in PBS and then blocked with 1% BSA in PBS. Primary antibody (R3195) was used in a concentration of 0.004–0.002 μg/μl. The primary antibody was visualized with FITC-conjugated anti–rabbit secondary antibody (Sigma Chemical Co.). Labeled specimens were examined with a confocal microscope (Insight Plus; Meridian Instruments, Inc., Okemos, MI) equipped with a krypton/argon mixed gas laser or with an MRC 1024 (Bio-Rad Laboratories, Melville, NY), also equipped with a krypton/argon mixed gas laser. Specimens were excited at 488 nm and observed at 522±13 nm to detect fluorescein. Images were reconstructed with Meridian IQ or Bio-Rad Lasersharp (version 3.0) software. CFTR immunofluorescence intensity in cross sections of tubular cells was quantified using a modified random line plot analysis described previously by Mattfeld et al. (24). Briefly, a template for the gray scale was established in preliminary experiments in basal perfused glands using the contrast enhancing mode of the NIH imaging software which assigns the brightest fluorescence detectable in the tubule a score of 255 and the least fluorescence detectable a value of 1. All tubules were normalized using this template in order to determine differences in cellular distribution of fluorescence between the experimental groups. Digitized

images were displayed on a screen using NIH imaging software (version 1.58b19), and tubule cross sections were overlaid with a grid containing 10 positions per tubular diameter. The placement of line plots on tubule cross sections was random, and signal intensity along these line plots was measured at 0.25-μm intervals. The first immunofluorescence signal detected at the lumen of the tubule on the line plot was defined as the border of the apical membrane. The last immunofluorescence signal extending into the cell was defined as the maximal cellular extension of CFTR. The cellular extension of CFTR immunofluorescence and maximal signal intensity under basal and stimulated conditions were compared using the unpaired *t* test and expressed as distance from apical membrane in micrometers ±SEM.

Results

Identification of CFTR in the shark rectal gland with antibody R3195. CFTR was identified in the rectal gland by Western blotting with R3195, a polyclonal rabbit antibody raised against a rodent 13–amino acid carboxy-terminal CFTR peptide, which differs from shark CFTR carboxy terminus by only four amino acids (18). In tissue from basal perfused glands (Fig. 1, lane *1*), this antibody recognizes a 155–165-kD broad band, and a less intense, slightly smaller 148-kD band. The amount of CFTR detected by Western blotting did not change after stimulation with three secretagogues: VIP, forskolin, and genistein (lanes *2–4*). A lysate of C127iWT1 cells stably expressing wild-type human CFTR (lane *5*) revealed a broad immunoreactive band (168–175 kD) and a smaller band with a similar molecular mass (148 kD) as detected in the rectal gland. Shark and rodent brain contain undetectable amounts of CFTR (lanes *6* and *7*). Preabsorption of the antibody with the synthetic peptide used for immunization eliminated all specific immunoreactivity (lane *8*).

To establish that R3195 specifically recognizes shark CFTR, we expressed shark CFTR cRNA in *Xenopus* oocytes, with water-injected oocytes as controls. 3 d after injection, oocytes were assessed with two-electrode voltage clamping to confirm functional expression of shark CFTR (see Methods). Cryosections of shark CFTR– and water-injected oocytes were then labeled with R3195 antibody and viewed by immunofluorescence alone (Fig. 2, *A*, *C*, and *E*) and immunofluorescence superimposed on transmission confocal micrographs (Fig. 2, *B*, *D*, and *F*). Oocytes expressing shark CFTR revealed bright immunoreactivity of the cell membrane, with considerable submembranous labeling (Fig. 2, *A* and *B*). Water-injected oocytes had no detectable CFTR immunoreactivity (Fig. 2, *C* and *D*). Immunoreactivity was not observed in shark CFTR–injected oocytes when antibody R3195 was preabsorbed with the peptide used to raise the antibody (Fig. 2, *E* and *F*).

Cellular localization of CFTR in basal and VIP-stimulated glands. Subcellular localization of CFTR was examined with R3195 in intact tubules under basal conditions and after stimulation with VIP (Fig. 3). In the basal state, there is well-defined apical CFTR labeling and diffuse intracellular labeling which extends midway into the cell, approaching the cell nucleus (Fig. 3 *A*). When CFTR immunofluorescence is superimposed on the transmission confocal image (Fig. 3 *B*), cellular detail is visible, including the apical membrane (*short arrow*), the basolateral membrane (*long arrow*), and nuclei. When the rectal gland is stimulated with VIP, a marked shift of CFTR towards the apical membrane is seen (Fig. 3, *C* and *D*). During stimulation, CFTR labeling is primarily apical, and there is almost complete loss of intracellular CFTR labeling.

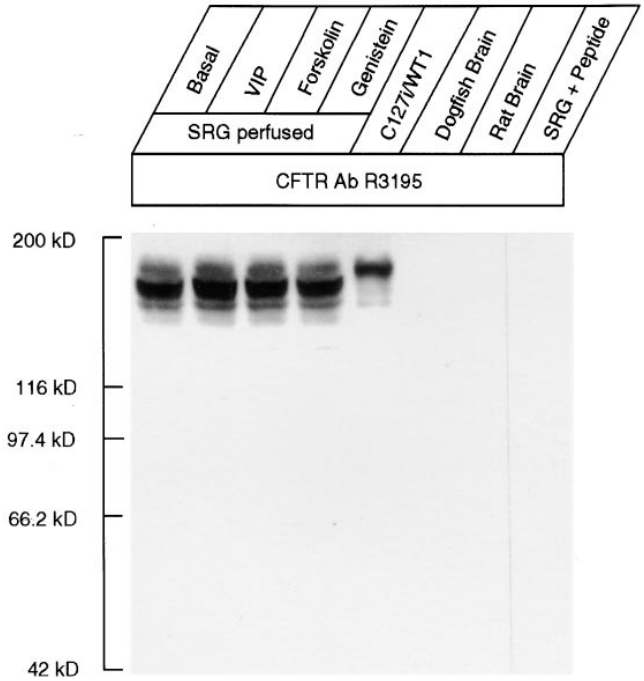

Figure 1. Western blot analysis of CFTR in the shark rectal gland. Tissue (25 μg protein each lane) and cell homogenate (10 μg protein) were separated electrophoretically on a 7.5% SDS-polyacrylamide gel and electrotransferred to Immobilon polyvinylidene difluoride transfer membranes. Membranes were then probed with CFTR antibody R3195 (lanes *1–7*) or probed separately in a 1:1 ratio with R3195 and the peptide which was used to raise the antibody (lane *8*). R3195 recognized a broad 165–155-kD band and a slightly smaller 148-kD band (lane *1*). The amount of CFTR did not change after short-term stimulation with VIP (lane *2*), forskolin (lane *3*), and genistein (lane *4*). A lysate of C127i cells stably expressing wild-type CFTR revealed a broad immunoreactive 175–168-kD band and a smaller band with the same molecular mass as recognized in the rectal gland (lane *5*). Dogfish brain (lane *6*) and rat brain (lane *7*) did not show immunoreactivity. Absorption of R3195 with the peptide used to raise the antibody fully abolished shark rectal gland (*SRG*) immunoreactivity (lane *8*).

Parallel measurements of chloride secretion and immunolocalization of CFTR in perfused rectal glands. Parallel measurements of chloride secretion and immunolocalization of CFTR by confocal microscopy were performed in perfused rectal glands in the basal state and during peak rates of secretion with three secretagogues, VIP, forskolin, and genistein. VIP binds to basolateral G protein–coupled receptors that increase intracellular cAMP and activate protein kinase A (25), and forskolin directly activates adenylate cyclase (26). Genistein is a tyrosine kinase inhibitor which activates Cl^- secretion by a cAMP-independent mechanism in the shark rectal gland (27) and other CFTR-expressing cells (28–31). In control glands perfused under basal conditions only, chloride secretion was low, declining to 151±65 μeq/h/g at 45 min (Fig. 4 *A*). The addition of VIP (10 nM) after 30 min of basal perfusion (chloride secretion 179±117 μeq/h/g) led to a 10-fold increase in peak Cl^- secretion (1,727±197 μeq/h/g, $n = 6$, $P < 0.001$, Fig. 4 *B*). Forskolin (10 μM) induced a sixfold increase in Cl^- secretion (197±28 vs. 1,239±67 μeq/h/g, $n = 6$, $P < 0.0001$, Fig. 4 *C*). Genistein increased secretion fourfold (147±70 vs. 541±70

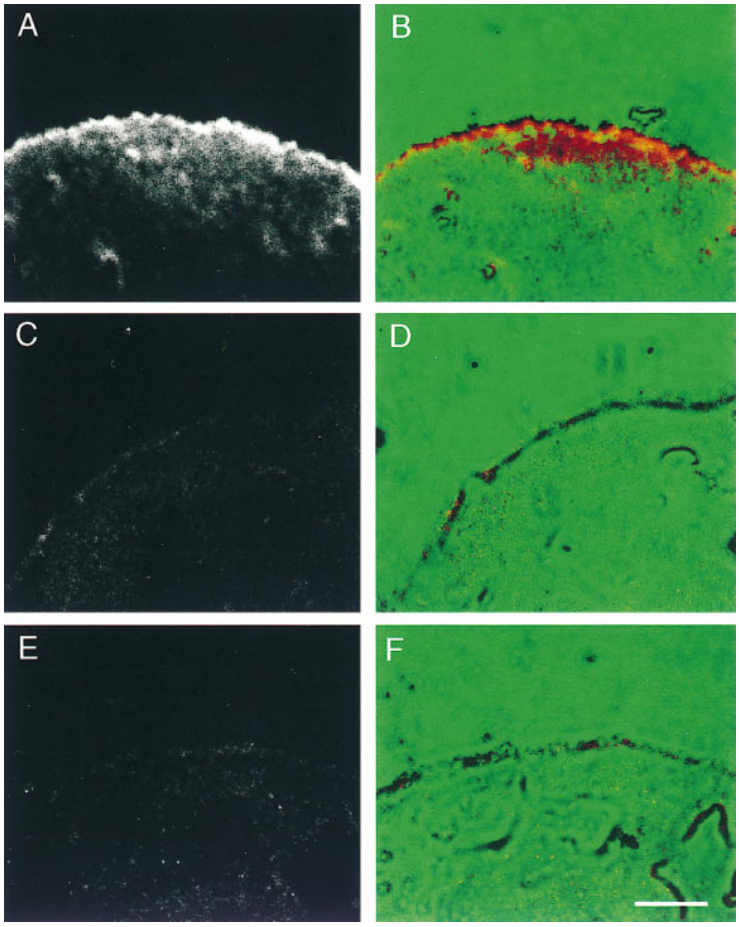

Figure 2. Specificity of antibody R3195 for shark CFTR. Oocytes were injected with shark CFTR cRNA or with water. After stimulation with forskolin to confirm functional CFTR expression, oocytes were frozen in liquid nitrogen, cryosectioned, fixed in ice-cold acetone, and labeled with R3195 as described in Methods. Staining with R3195 in shark CFTR–injected oocytes resulted in intense membrane and submembranous labeling (*A*). To visualize the cellular borders of the oocyte, CFTR labeling (*red*) is superimposed on the transmission confocal micrograph (*B*). No CFTR labeling was observed in water-injected oocytes (*C* and *D*). Immunofluorescence labeling in shark CFTR–injected oocytes was blocked by preabsorbing R3195 antibody before the incubation with the corresponding peptide used to raise the antibody (*E* and *F*). Scale bar for all photomicrographs, 100 μm (*right lower corner*, *F*).

μeq/h/g, $n = 6$, $P < 0.01$, Fig. 4 *D*). Tissue for CFTR immunolocalization was obtained at 45 min of basal perfusion and during peak rates of secretion for VIP, forskolin, and genistein.

Immunolocalization of CFTR with antibody R3195 in basal perfused glands revealed a deep extension of CFTR staining into tubular cells, extending from the apical membrane midway into the cell, often to the cell nucleus (Fig. 4 *E*). Stimulation of chloride secretion with VIP, forskolin, and genistein was associated with a marked decrease in intracellular CFTR staining and more distinct staining of the apical membrane (Fig. 4, *F*, *G*, and *H*). Similar labeling was observed when glands were fixed with 4% paraformaldehyde (data not shown).

Quantification of CFTR signal intensity and extension of CFTR into tubular cells in glands perfused under basal and stimulated conditions. We next applied stereological methods to quantify the signal intensity and cellular extension of CFTR immunoreactivity in basal and stimulated glands. CFTR immunofluorescence intensity in cross sections of tubular cells was quantified using a grid containing 10 positions per tubular diameter, and signal intensity was measured at 0.25-μm intervals (see Methods). The first immunofluorescence signal detected at the lumen of the tubule on the line plot was defined as the border of the apical membrane. We analyzed the signal intensity of CFTR labeling over the cellular diameter in 23–26 tubular cells under each condition (basal, VIP, forskolin, and genistein stimulation; $n = 4$–5 glands per group). The resulting curves were averaged and plotted as shown in Fig. 5. Under basal conditions, the curve displays a moderately steep initial slope, and a gradual intracellular decline (Fig. 5 *A*). In basal glands, the maximal extension of CFTR from the apical membrane into the cell averaged 7.28±0.35 μm (Fig. 5 *A*). VIP, forskolin, and genistein caused a steeper initial slope as well as a substantially steeper intracellular decline (Fig. 5, *B–D*). The maximal extension of CFTR into the cell averaged 3.24±0.08 μm for VIP, 4.08±0.13 μm for forskolin, and 3.19±0.1 μm for genistein ($P < 0.001$ for each compared with basal conditions). Moreover, the peak intensity of CFTR fluorescence shifted towards the apical membrane (peak fluorescence 2.5±0.13 μm in basal glands vs. 1.51±0.06, 1.77±0.1, and 1.38±0.05 μm in VIP, forskolin, and perfused glands, respectively; $P < 0.001$ for each compared with basal).

Reversibility of CFTR trafficking after withdrawing of secretagogue. To investigate the reversibility of CFTR trafficking to the apical membrane, we stimulated glands with VIP and then removed the secretagogue and obtained frozen sections for immunocytochemistry. As shown in Fig. 6 *A*, chloride secretion rose to 2,621±357 μeq/h/g after stimulation with VIP (10 nM), and declined to basal values (50±28 μeq/h/g) during 30 min of basal perfusion after removal of VIP. Fig. 6 *B* depicts the cellular distribution of CFTR during this time course. Under basal conditions, CFTR resides at both intracellular sites and apical regions with a mean CFTR signal extension of 7.52±0.42 μm ($n = 14$) (Fig. 6 *B*, *graph*). VIP caused a significant shift towards the apical membrane, with a significant re-

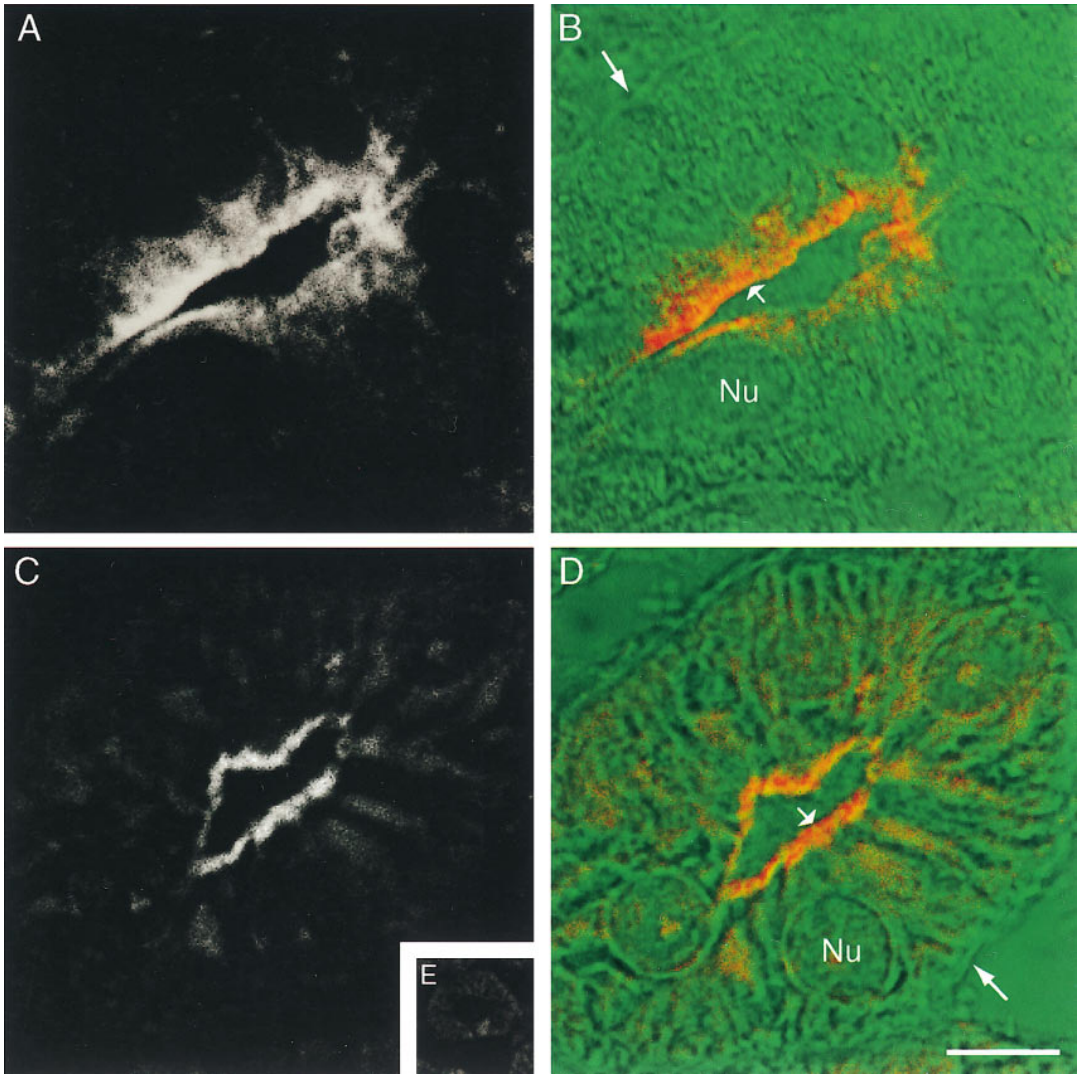

Figure 3. Cellular CFTR immunolocalization under basal and stimulated conditions. Shark rectal glands were perfused under basal conditions or stimulated with VIP 10 nM. After perfusion, glands were frozen, and cryosections were obtained and labeled for CFTR as described in Methods. Under basal conditions, the CFTR signal extends far into the cell (*A*). CFTR (*red*) is superimposed on the confocal transmission micrograph to illustrate cellular detail, including apical membrane (*short arrow*), basolateral membrane (*long arrow*), and a nucleus (*Nu*) (*B*). Stimulation with VIP led to a dramatic condensation of the CFTR signal at the apical membrane (*C*). In the transmission confocal micrograph (*D*), immunofluorescence is superimposed to demonstrate localization of CFTR at the apical membrane (*short arrow*). A nucleus (*Nu*) and the basolateral membrane (*long arrow*) are also marked. Preabsorption of R3195 with the corresponding peptide used to raise the antibody abolished immunofluorescence (*E*). Scale bar for all photomicrographs, 10 μm (*right lower corner*, *D*).

duction of the mean CFTR signal extension, to 3.42±0.25 μm ($P < 0.01$, $n = 14$). After removal of VIP, a significant redistribution of CFTR to intracellular sites occurred, with a mean CFTR signal extension of 6.5±0.3 μm ($P < 0.01$, $n = 24$).

Measurements of cellular diameter and surface area in basal and stimulated glands. To investigate whether the observed changes in CFTR labeling could be due to changes in cell shape and/or surface area, we estimated cellular diameter and cellular surface area at the same level of resolution used for immunofluorescence measurements. Cell diameter was determined by overlaying a line plot on a transmission confocal micrograph and measuring the distance between the apical and basolateral membrane. Cellular surface area was estimated by tracing the cellular border in transmission confocal micrographs and integrating the delineated surface. The mean cellular diameter was 19.8±0.8, 18.2±0.7, 19.3±0.9, and 19.7±0.6 μm under basal, VIP-, forskolin-, and genistein-stimulated conditions, respectively (Table I). Cellular surface area also did not change with stimulation compared with basal conditions (Table I). We conclude that changes in cellular diameter and surface area, as detected by transmission confocal microscopy, do not account for the significant shift in CFTR immunoreactivity towards the apical membrane upon stimulation. Our observation is consistent with findings of Lytle and Forbush (32), who reported no changes in cell volume of rectal gland tubules during forskolin-stimulated secretion using gravimetric techniques. Using higher resolution techniques (measurement of membrane capacitance and electron microscopy), Takahaschi et al. (33) have shown that secretagogues increase membrane area in CFTR expressing *Xenopus* oocytes as a consequence of increased vesicular trafficking. This change, if present in rectal gland cells, is not detectable at the level of transmission confocal microscopy.

Discussion

Our studies provide the first morphological evidence in an intact tissue that acute hormonal stimulation of chloride trans-

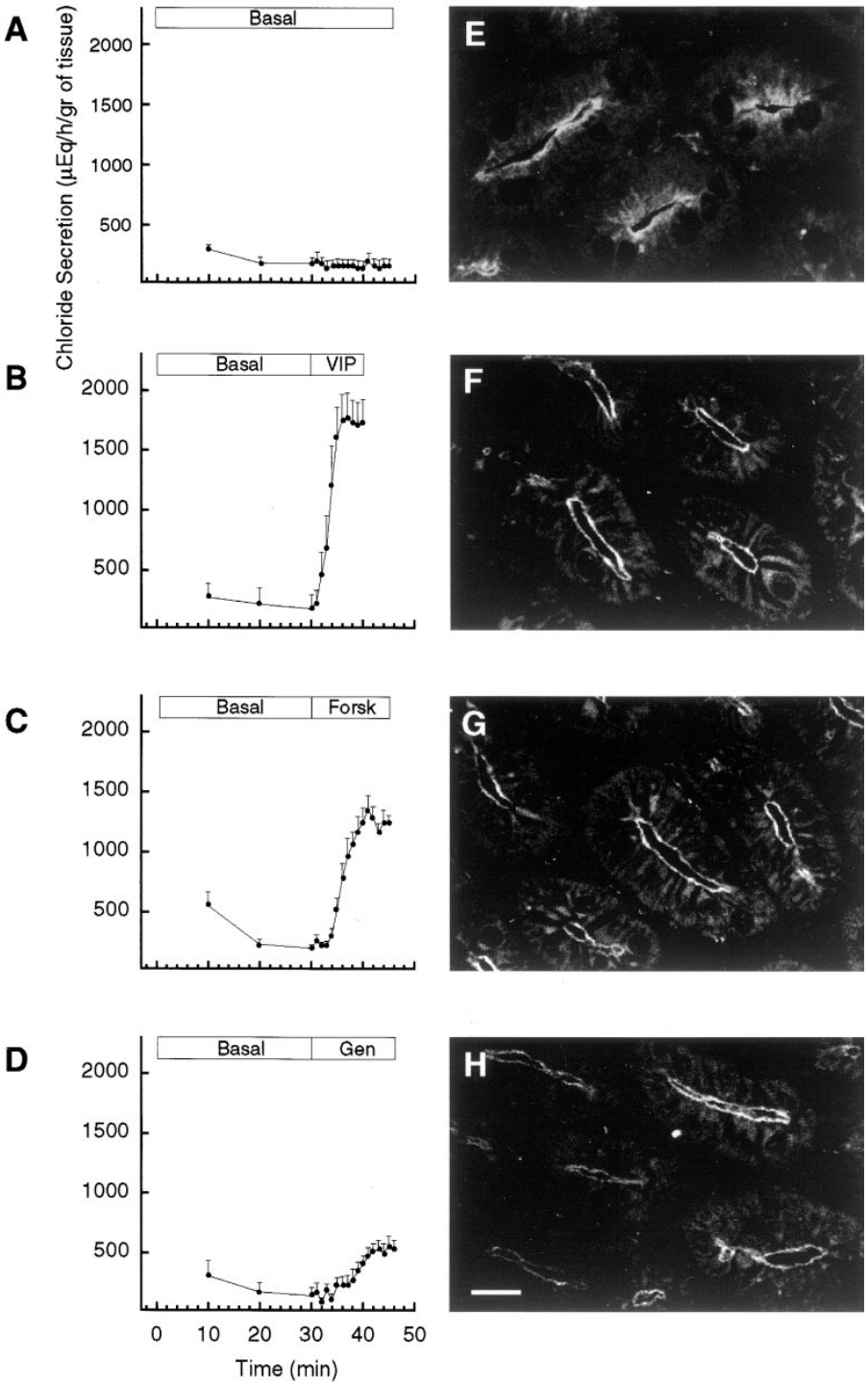

Figure 4. Chloride secretion and immunolocalization of CFTR in perfused rectal glands. All rectal glands were perfused with shark Ringer's solution for 30 min to achieve basal levels of Cl^- secretion. Glands were then perfused for an additional 15 min in unstimulated basal controls (*A*), with 10 nM VIP (*B*), 10 μM forskolin (*C*, *Forsk*), or 100 μM genistein (*D*, *Gen*). Tissue for CFTR immunolocalization was obtained at 45 min of basal perfusion and during peak rates of secretion (10, 15, and 17 min) for VIP, forskolin, and genistein, respectively. Glands were snap-frozen in liquid nitrogen immediately after the experiments, and cryosections were fixed in acetone at −24°C and stained for CFTR with the polyclonal antiserum R3195. Primary antibody was visualized with FITC-conjugated goat anti–rabbit antibody. CFTR was localized at the apical pole of the tubular cells (*E*) with immunofluorescence extending deeply into the cell. VIP-induced (*F*) staining is sharply localized to the apical pole of the tubular cell. Forskolin (*G*) and genistein (*H*) induced similar CFTR staining patterns. Scale bar, 25 μm.

port is accompanied by trafficking of CFTR from intracellular compartments to the apical membrane. First, we established the specificity of antibody R3195 used in these studies. In a previous study, R3195 detected CFTR in a Western blot analysis in +/+ wild-type mice and failed to detect CFTR in −/− CFTR knockout mice (22). Using R3195 in the rectal gland, CFTR was identified by Western blotting as a doublet weighing 165–155 and 148 kD, consistent with fully glycosylated CFTR and deglycosylated lower molecular mass species (5, 34). This molecular mass is in agreement with Marshall et al. (18), who cloned shark CFTR. Preabsorption with peptide abolished all R3195 immunoreactivity in both Western blots and tissue sections. In the rectal gland we also observed similar CFTR immunolocalization and Western blots using a second antibody, α 1468 (35), a well-characterized antibody against carboxy-terminal human CFTR (4, 5).

To establish the specificity of antibody R3195 for shark CFTR, we expressed shark CFTR cRNA in *Xenopus* oocytes. R3195 prominently labeled both membranous and submembranous shark CFTR, and this immunofluorescence was abol-

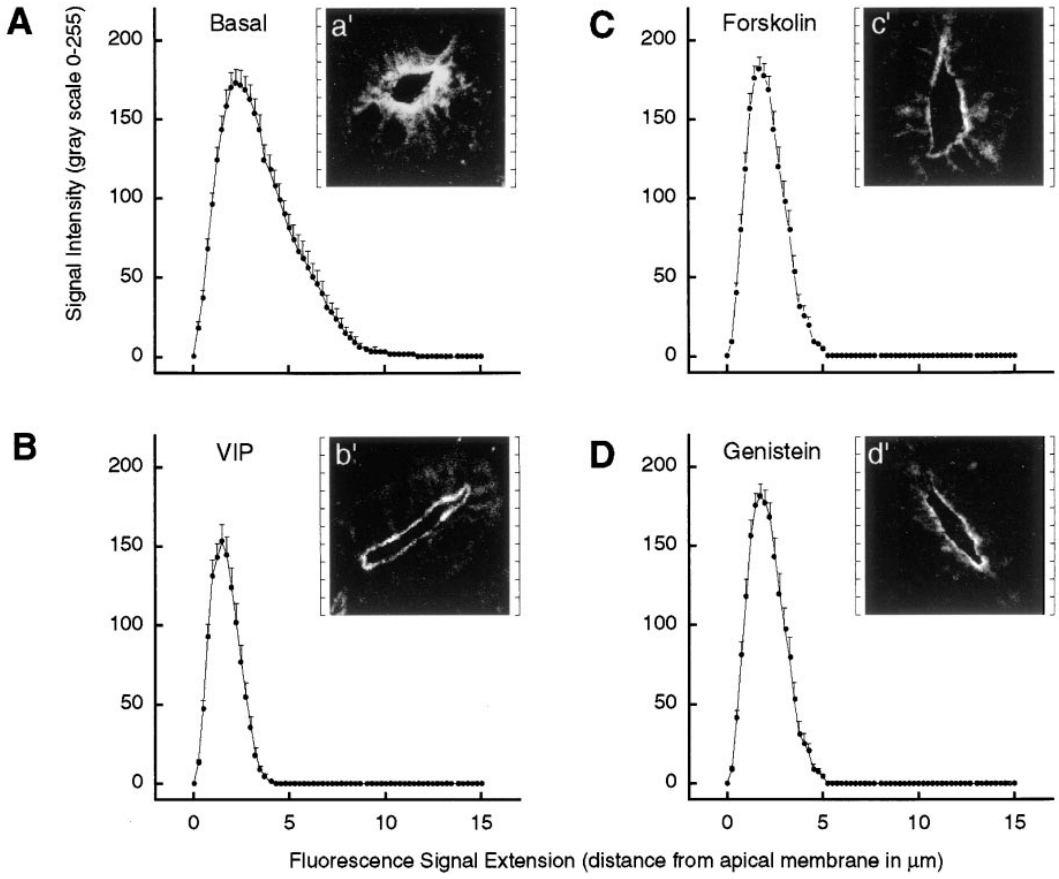

Figure 5. Quantification of CFTR signal extension under basal and stimulated conditions in perfused shark rectal glands. An analysis of the signal intensity of CFTR labeling over the cellular diameter in 23–26 tubular cells under each condition (basal, VIP-, forskolin-, and genistein-stimulated) was performed in glands from three to five sharks per group. Tubule cross sections were overlaid with a grid containing 10 positions per tubular diameter. The placement of line plots on tubule cross sections was random, and signal intensity along line plots was measured at 0.25-μm intervals (see Methods). In basal glands (*A*), the maximal extension of CFTR from the apical membrane into the cell averaged 7.28±0.35 μm. VIP (*B*), forskolin (*C*), and genistein (*D*) caused a steeper initial slope, a substantially steeper intracellular decline, and significant reduction in maximal extension of CFTR into the cell. *Insets*, A single representative tubule under basal (*a′*), VIP-stimulated (*b′*), forskolin-stimulated (*c′*), and genistein-stimulated (*d′*) conditions.

ished when the R3195 was preabsorbed with peptide. R3195 failed to detect immunofluorescence in control water-injected oocytes.

We used this antibody in parallel experiments in the shark rectal gland to quantify chloride secretion and CFTR immunofluorescence. When chloride secretion was acutely stimulated with diverse secretagogues, three quantitative changes were observed: (*a*) the extension of CFTR from the apical membrane into the cell decreased abruptly; (*b*) the peak intensity of CFTR fluorescence shifted towards the apical membrane; (*c*) after removal of secretagogue (VIP), both Cl^- secretion and CFTR immunofluorescence extension reversed in parallel to basal values. We interpret these findings as compelling evidence that CFTR traffics to the apical membrane during hormonal stimulation of chloride secretion in the rectal gland. Our data strongly support the concept that under physiological conditions, intracellular CFTR shifts to the apical membrane, and that secretagogue-stimulated insertion of CFTR-containing vesicles leads to an increase in chloride transport.

Table I. Cellular Diameter and Surface Area under Basal and Stimulated Conditions Obtained by Transmission Confocal Microscopy

Condition	Cellular diameter	Cellular surface	*n**
	μm	*μm²*	
Basal	19.8±0.8	243.9±6.3	16
VIP	18.2±0.7	250.9±11.1	15
Forskolin	19.3±0.9	236.4±17.7	15
Genistein	19.7±0.6	244.1±13.3	15

*Number of tubular cells examined.

Although evidence supporting this hypothesis has been accumulating, acceptance of this view has been opposed by numerous contradictory studies, particularly in the T84 cell line. Movement of vesicles from the perinuclear area to the cell periphery was observed in T84 cells in response to secretagogues and was accompanied by a threefold increase in de novo microvilli formation after stimulation with forskolin (36). Bradbury et al. (8) found that cAMP increases exocytosis in pancreatic adenocarcinoma cells stably transfected with CFTR, but not in cells with the ΔF508 CFTR mutation. Schwiebert et al. (9) showed that cAMP increases Cl^- conductance, membrane capacitance, and FITC-labeled dextran exocytosis in transformed airway epithelial cells expressing CFTR. However, in three cell lines expressing endogenous CFTR (T84 cells, Caco2, and HT29 clone 19A), Denning et al. (10) found that maneuvers that increase cAMP (forskolin and 3-isobutyl-1-methyl xanthine) did not alter the staining pattern for CFTR. Using T84 cells, Prince et al. (11) also found that treatment with forskolin did not increase the relative amounts of

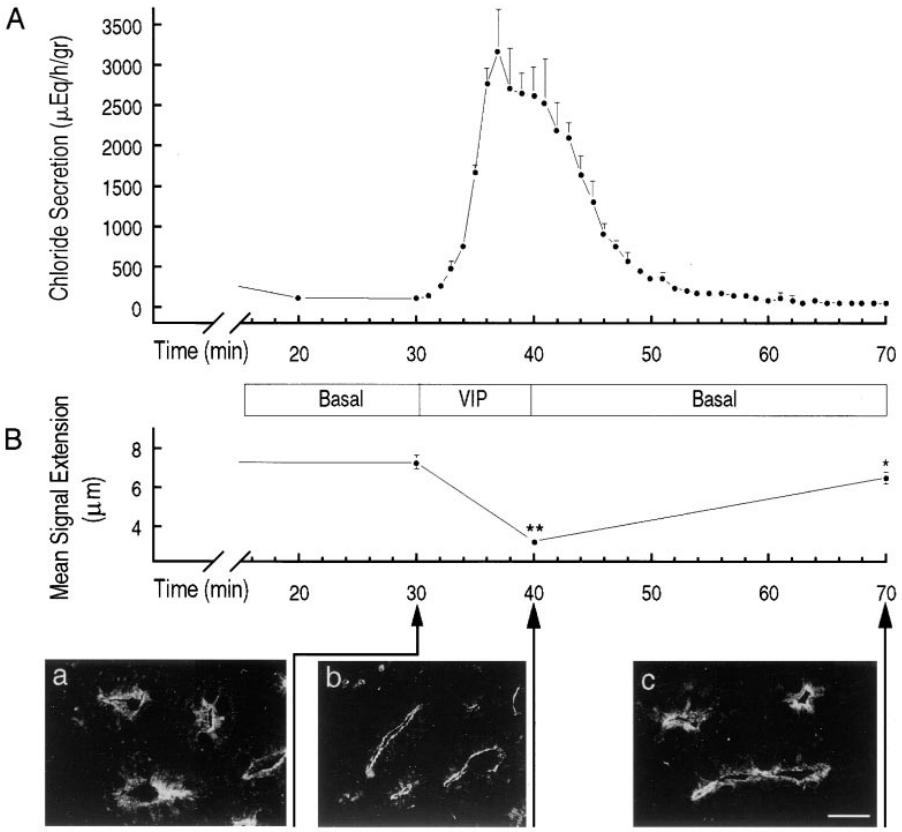

Figure 6. Parallel reversal of chloride secretion and CFTR trafficking after VIP. Glands were perfused under basal conditions for 30 min, then stimulated with VIP (10 nM) for 10 min, followed by a 30-min perfusion without VIP. (*A*) Stimulation with VIP led to a significant increase in chloride secretion. After withdrawal of VIP at 40 min, chloride secretion returned to basal values. (*B*) CFTR immunolocalization was determined after 30 min of basal perfusion (*a*), after 10 min of stimulation with VIP (*b*), and 30 min after removal of the hormone (*c*) ($n = 3$ for each condition). (*Top*) Graph illustrates mean CFTR signal extension from the apical membrane at the three different time points. During stimulation with VIP, there is a significant decrease in the mean CFTR signal extension. After removal of the hormone, a significant redistribution of the CFTR signal to basal values occurs. (*Bottom*) CFTR immunofluorescence micrographs illustrate CFTR localization after 30 min of basal perfusion (*a*), during stimulation with VIP (*b*), and after removal of VIP (*c*). Scale bar for all photomicrographs, 20 μm (*right lower corner*, *c*).

CFTR in the apical membranes. Santos and Reenstra (37) compared the dose-dependence of forskolin- and 8 chlorophenylthio-cAMP–induced inhibition of endocytosis with the dose-dependence of chloride channel activation in both T84 cells and the tracheal cell line 9HTE and concluded that cAMP did not regulate membrane trafficking. In Chinese hamster ovary cells expressing CFTR, Dho et al. (12) found no evidence that cAMP regulated exocytosis or endocytosis.

These conflicting results argue for examining this question in native physiological tissues that possess all necessary elements required for acute regulation of membrane trafficking. Our findings in the shark rectal gland provide strong morphological evidence that secretagogues acutely regulate the trafficking of CFTR. Two recent studies in nonnative systems support this conclusion. Tousson et al. (13) reported a twofold increase in relative CFTR immunofluorescence at the apical membrane of T84 cell monolayers after addition of forskolin. Using *Xenopus* oocytes expressing human CFTR, Takahaschi et al. (33) demonstrated recently that stimulation of chloride current by cAMP was intimately linked in a saturable manner to an increase in membrane area determined both morphologically and by membrane capacitance measurements. A limitation of the present study is that the number of channels localized to the apical membrane after stimulation was not quantitated. Additional studies, such as immuno-gold labeling, are required to demonstrate that the number of CFTR channels at the apical membrane surface of rectal gland tubules increases with hormone treatment.

Forskolin, VIP, and genistein caused comparable shifts of CFTR towards the apical membrane, but the secretory response to genistein was less than that observed with forskolin or VIP. The reason for this is not clear, but may be related to the cAMP-independent mechanism by which genistein activates chloride secretion. In each epithelial system examined, Cl^- secretion with genistein does not reach the maximal values achieved with forskolin (27, 28, 30). It is possible that genistein selectively activates CFTR trafficking, in contrast to phosphorylation-induced increases in the open probability (P_o) of membrane resident CFTR chloride channels, but our data do not address this issue.

The acute recruitment of transporters in the membrane via exocytotic insertion and their removal via endocytotic retrieval has now been established for several transport proteins in native tissues. Vasopressin-sensitive water transport is dependent on aquaporin-2 water channels shuttling in aggrephores to the apical membrane of vasopressin-responsive cells (38, 39). In adipocytes, Glut4 is moved from subcellular organelles to the cell surface when insulin-sensitive glucose transport is initiated (40, 41). Similar observations have been made in studies of acid secretion via the H^+ pump (42). However, there has been no previous morphological evidence that ion channels undergo similar translocation in response to hormones.

In summary, we present the first morphological evidence in an epithelial organ that CFTR translocates from intracellular sites to the apical membrane after hormonal stimulation. These findings strongly support a dual role for secretagogues in stimulating chloride secretion: acute recruitment of CFTR from intracellular sites to the apical membrane, and phosphorylation-mediated regulation of channels residing in the membrane.

Acknowledgments

The authors thank L. Matthews, C. Smith, P. Schwartz, and G. Forrest for excellent technical assistance, and Mrs. Ramona Gregg for help in preparing the manuscript. The authors are grateful to Dr. J. Henson and Dr. C. Lindschau for expert assistance with imaging techniques, and to Dr. H.F. Cantiello for providing C127iWT1 cells.

This work was supported by National Institutes of Health grants DK-34208 and P30-ES-3828 (Center for Membrane Toxicology Studies), American Heart Association grant 9607741S to J.N. Forrest, and Cystic Fibrosis Foundation and Department of Veterans Affairs Merit Review to C.R. Marino.

References

1. Kerem, B., J.M. Rommens, J.A. Buchanan, D. Markiewicz, T.K. Cox, A. Chakravarti, M. Buchwald, and L.C. Tsui. 1989. Identification of the cystic fibrosis gene: genetic analysis. *Science.* 245:1073–1080.

2. Kartner, N., O. Augustinas, T.J. Jensen, A.L. Naismith, and J.R. Riordan. 1992. Mislocalization of delta F508 CFTR in cystic fibrosis sweat gland. *Nat. Genet.* 1:321–327.

3. Dalemans, W., J. Hinnrasky, P. Slos, D. Dreyer, C. Fuchey, A. Pavirani, and E. Puchelle. 1992. Immunocytochemical analysis reveals differences between the subcellular localization of normal and delta Phe508 recombinant cystic fibrosis transmembrane conductance regulator. *Exp. Cell Res.* 201:235–240.

4. Marino, C.R., L.M. Matovcik, F.S. Gorelick, and J.A. Cohn. 1991. Localization of the cystic fibrosis transmembrane conductance regulator in pancreas [published erratum appears in *J. Clin. Invest.* 1991. 88:1433]. *J. Clin. Invest.* 88: 712–716.

5. Cohn, J.A., A.C. Nairn, C.R. Marino, O. Melhus, and J. Kole. 1992. Characterization of the cystic fibrosis transmembrane conductance regulator in a colonocyte cell line. *Proc. Natl. Acad. Sci. USA.* 89:2340–2344.

6. Webster, P., L. Vanacore, A.C. Nairn, and C.R. Marino. 1994. Subcellular localization of CFTR to endosomes in a ductal epithelium. *Am. J. Physiol.* 267:C340–C348.

7. Bradbury, N.A., J.A. Cohn, C.J. Venglarik, and R.J. Bridges. 1994. Biochemical and biophysical identification of cystic fibrosis transmembrane conductance regulator chloride channels as components of endocytic clathrin-coated vesicles. *J. Biol. Chem.* 269:8296–8302.

8. Bradbury, N.A., T. Jilling, G. Berta, E.J. Sorscher, R.J. Bridges, and K.L. Kirk. 1992. Regulation of plasma membrane recycling by CFTR. *Science.* 256: 530–532.

9. Schwiebert, E.M., F. Gesek, L. Ercolani, C. Wjasow, D.C. Gruenert, K. Karlson, and B.A. Stanton. 1994. Heterotrimeric G proteins, vesicle trafficking, and CFTR Cl-channels. *Am. J. Physiol.* 267:C272–C281.

10. Denning, G.M., L.S. Ostedgaard, S.H. Cheng, A.E. Smith, and M.J. Welsh. 1992. Localization of cystic fibrosis transmembrane conductance regulator in chloride secretory epithelia. *J. Clin. Invest.* 89:339–349.

11. Prince, L.S., A. Tousson, and R.B. Marchase. 1993. Cell surface labeling of CFTR in T84 cells. *Am. J. Physiol.* 264:C491–C498.

12. Dho, S., S. Grinstein, and J.K. Foskett. 1993. Plasma membrane recycling in CFTR-expressing CHO cells. *Biochim. Biophys. Acta.* 1225:78–82.

13. Tousson, A., C.M. Fuller, and D.J. Benos. 1996. Apical recruitment of CFTR in T84 cells is dependent on cAMP and microtubules but not Ca2+ or microfilaments. *J. Cell Sci.* 109:1325–1334.

14. Forrest, J.N. 1996. Cellular and molecular biology of chloride secretion in the shark rectal gland: regulation by adenosine receptors. *Kidney Int.* 49: 1557–1562.

15. Silva, P., R.J. Solomon, and F.H. Epstein. 1996. The rectal gland of *Squalus acanthias*: a model for the transport of chloride. *Kidney Int.* 49:1552–1556.

16. Eveloff, J., R. Kinne, E. Kinne-Saffran, H. Murer, P. Silva, F.H. Epstein, J. Stoff, and W.B. Kinter. 1978. Coupled sodium and chloride transport into plasma membrane vesicles prepared from dogfish rectal gland. *Pflugers Arch.* 378:87–92.

17. Lytle, C., and B. Forbush 3d. 1992. The Na-K-Cl cotransport protein of shark rectal gland. II. Regulation by direct phosphorylation. *J. Biol. Chem.* 267: 25438–25443.

18. Marshall, J., K.A. Martin, M. Picciotto, S. Hockfield, A.C. Nairn, and L.K. Kaczmarek. 1991. Identification and localization of a dogfish homolog of human cystic fibrosis transmembrane conductance regulator. *J. Biol. Chem.* 266:22749–22754.

19. Devor, D.C., J.N. Forrest, Jr., W.K. Suggs, and R.A. Frizzell. 1995. cAMP-activated Cl− channels in primary cultures of spiny dogfish (*Squalus acanthias*) rectal gland. *Am. J. Physiol.* 268:C70–C79.

20. Kelley, G.G., E.M. Poeschla, H.V. Barron, and J.N. Forrest, Jr. 1990. A1 adenosine receptors inhibit chloride transport in the shark rectal gland. Dissociation of inhibition and cyclic AMP. *J. Clin. Invest.* 85:1629–1636.

21. Kelley, G.G., O.S. Aassar, and J.N. Forrest, Jr. 1991. Endogenous adenosine is an autacoid feedback inhibitor of chloride transport in the shark rectal gland. *J. Clin. Invest.* 88:1933–1939.

22. French, P.J., J.H. van Doorninck, R.H. Peters, E. Verbeek, N.A. Ameen, C.R. Marino, H.R. de Jonge, J. Bijman, and B.J. Scholte. 1996. A delta F508 mutation in mouse cystic fibrosis transmembrane conductance regulator results in a temperature-sensitive processing defect in vivo. *J. Clin. Invest.* 98:1304–1312.

23. Kozak, M. 1984. Compilation and analysis of sequences upstream from the translational start site in eukaryotic mRNAs. *Nucleic Acids Res.* 12:857–872.

24. Mattfeld, T., G. Mall, A. Von Herbay, and P. Moeller. 1989. Stereological investigation of anisotropic structures with the orientator. *Acta Stereol.* 8:671–676.

25. Stoff, J.S., R. Rosa, R. Hallac, P. Silva, and F.H. Epstein. 1979. Hormonal regulation of active chloride transport in the dogfish rectal gland. *Am. J. Physiol.* 237:F138–F144.

26. Seamon, K.B., and J.W. Daly. 1986. Forskolin: its biological and chemical properties. *Adv. Cyclic Nucleotide Protein Phosphorylation Res.* 20:1–150.

27. Lehrich, R.W., and J.N. Forrest. 1995. Tyrosine phosphorylation is a novel pathway for regulation of chloride secretion in the shark rectal gland. *Am. J. Physiol.* 269:F594–F600.

28. Illek, B., H. Fischer, G.F. Santos, J.H. Widdicombe, T.E. Machen, and W.W. Reenstra. 1995. cAMP-independent activation of CFTR Cl channels by the tyrosine kinase inhibitor genistein. *Am. J. Physiol.* 268:C886–C893.

29. Illek, B., H. Fischer, and T.E. Machen. 1996. Alternate stimulation of apical CFTR by genistein in epithelia. *Am. J. Physiol.* 270:C265–C275.

30. Reenstra, W.W., K. Yurko-Mauro, A. Dam, S. Raman, and S. Shorten. 1996. CFTR chloride channel activation by genistein: the role of serine/threonine protein phosphatases. *Am. J. Physiol.* 271:C650–C657.

31. Sears, C.L., F. Firoozmand, A. Mellander, F.G. Chambers, I.G. Eromar, A.G. Bot, B. Scholte, H.R. De Jonge, and M. Donowitz. 1995. Genistein and tyrphostin 47 stimulate CFTR-mediated Cl− secretion in T84 cell monolayers. *Am. J. Physiol.* 269:G874–G882.

32. Lytle, C., and B. Forbush 3d. 1992. Na-K-Cl cotransport in the shark rectal gland. II. Regulation in isolated tubules. *Am. J. Physiol.* 262:C1009–C1017.

33. Takahaschi, A., S.C. Watkins, M. Howard, and R.A. Frizzell. 1996. CFTR-dependent membrane insertion is linked to stimulation of the CFTR chloride conductance. *Am. J. Physiol.* 271:C1887–C1894.

34. Cheng, S.H., R.J. Gregory, J. Marshall, S. Paul, D.W. Souza, G.A. White, C.R. O'Riordan, and A.E. Smith. 1990. Defective intracellular transport and processing of CFTR is the molecular basis of most cystic fibrosis. *Cell.* 63: 827–834.

35. Lehrich, R.W., C. Marino, H. Henschel, C. Kelmenson, M. Ratner, and J.N. Forrest. 1995. Immunolocalization of DFTR with the rodent CFTR antibody R3195 in the rectal gland of the dogfish shark, *Squalus acanthias. Bull. Mt. Desert Isl. Biol. Lab.* 35:28–31.

36. Sorscher, E.J., C.M. Fuller, R.J. Bridges, A. Tousson, R.B. Marchase, B.R. Brinkley, R.A. Frizzell, and D.J. Benos. 1992. Identification of a membrane protein from T84 cells using antibodies made against a DIDS-binding peptide. *Am. J. Physiol.* 262:C136–C147.

37. Santos, G.F., and W.W. Reenstra. 1994. Activation of the cystic fibrosis transmembrane regulator by cyclic AMP is not correlated with inhibition of endocytosis. *Biochim. Biophys. Acta.* 1195:96–102.

38. Kachadorian, W.A., S.D. Levine, J.B. Wade, V.A. DiScala, and R.M. Hays. 1977. Relationship of aggregated intramembranous particles to water permeability in vasopressin-treated toad urinary bladder. *J. Clin. Invest.* 59: 576–581.

39. Deen, P.M., H. Croes, R.A. van Aubel, L.A. Ginsel, and C.H. van Os. 1995. Water channels encoded by mutant aquaporin-2 genes in nephrogenic diabetes insipidus are impaired in their cellular routing. *J. Clin. Invest.* 95:2291–2296.

40. Cushman, S.W., and L.J. Wardzala. 1980. Potential mechanism of insulin action on glucose transport in the isolated rat adipose cell. *J. Biol. Chem.* 255:4758–4762.

41. Kono, T., K. Suzuki, E. Dansey, W. Robinson, and T.L. Belvins. 1981. Energy-dependent and protein synthesis-independent recycling of the insulin-sensitive glucose transport mechanism in fat cells. *J. Biol. Chem.* 256:6400–6407.

42. Brown, D., S. Gluck, and J. Hartwig. 1987. Structure of the novel membrane-coating material in proton-secreting epithelial cells and identification as an H+ATPase. *J. Cell Biol.* 105:1637–1648.